Velocity correlated multifragmentation in C_{60}-surface impact: Energy distributions and incidence angle dependences

A. Kaplan,[1] A. Bekkerman,[2] B. Tsipinyuk,[2] and E. Kolodney[2]
[1]*School of Physics and Astronomy, University of Birmingham, Birmingham B15 2TT, United Kingdom*
[2]*Schulich Department of Chemistry, Technion–Israel Institute of Technology, Haifa 32000, Israel*
(Received 22 September 2010; published 15 December 2010)

We have studied surface impact multifragmentation of C_{60}^- following subkiloelectron volt, near-grazing collision with a nickel target. Field free, mass resolved kinetic energy distributions and incidence angle dependences were measured for the outgoing C_n^- ($n=2-15$) fragments. All energy distributions could be described within a scenario where C_n groups are statistically (thermally) emitted off an outgoing precursor away from the surface, as manifested by shifted Maxwellian flux distributions with only two parameters: kinetic energy ε (per carbon atom) associated with the center-of-mass velocity of the moving precursor and its temperature T. The best fitted parameters were found to be $\varepsilon=2.60$ eV and $kT=0.86$ eV. A distinct narrowing effect was observed for the incidence angle dependences of the C_n^- fragments yield, going from C_4^- to C_{15}^-. The gradually decreasing angular width as a function of cluster size n was analyzed based on the assumption of isotropic, statistical fragments emission off an outgoing multifragmenting source (the superhot precursor). The predicted $1/\sqrt{n}$ narrowing law was found to be in good agreement with the observed width effect and the two parameters ε, kT extracted from the independently measured kinetic-energy distributions. We conclude that both energy and angle distributions clearly demonstrate a statistical expansionlike, precursor-mediated multifragmentation mechanism.

DOI: 10.1103/PhysRevB.82.245421 PACS number(s): 68.49.Df, 36.40.Qv, 34.50.−s

I. INTRODUCTION

Multifragmentation phenomena where highly energized complex and finite system instantaneously disintegrates into several of its constituents are important in many fields and are sometimes of a universal nature regarding general patterns which may be revealed. Once the deposited energy exceeds that corresponding to the evaporation regime (sequential emission of elementary subunits) approaching the total cohesion energy of the system, multifragmentation dynamics will start to dominate, eventually reaching complete disintegration of the system into its smallest units (the shattering limit). This multiparticle break-up behavior was observed over extremely broad size scale ranging from macroscopic objects,[1] through large clusters and molecules and down to superhot atomic nuclei.[2,3] Actually, the subject was most intensively studied, both experimentally and theoretically, in the context of nuclear multifragmentation following heavy ions collisions and hadron-nucleus collisions in the range of 3–10 MeV/nucleon where both statistical and dynamical models are used to describe experimental results.[2,3] Multifragmentation of atomic nuclei is often treated in terms of liquid-gaslike (or "liquid-fog") phase transition based on a microcanonical thermodynamic approach.[4] Multifragmentation phenomena for polyatomic molecular/cluster species were mainly studied following impulsive surface impact excitation in the shattering limit, namely, complete disintegration into elementary subunits.[5–7] The projectiles included weakly bound clusters such as $(NH_3)_nH^+$ ($n=4-40$) (Ref. 7) and $I_2(CO_2)_n^-$ ($n=1-50$) (Ref. 8) where the total binding energy could easily be exceeded by the impact-induced internal excitation as well as tightly bound molecular ions such as Sb_n^+ ($n=3-12$),[9] $Si(CD_3)_3^+$,[10] peptide ions,[11] and fullerenes.[12,13] The main experimental evidence in these studies was the observation of the so-called shattering transition based on a relatively sharp (in impact energy) variation in mass abundances from the parent to many small(est) subunits but usually without detailed analysis of mass resolved energy and angle distributions which can reveal fragment size-dependent correlations. This was also associated with the underlying assumption that the shattering event is necessarily completed "at the surface" and "during collision" while all fragments are still in close contact with each other and with the surface (strong surface interaction regime) implying energy equalization between all emitted fragments with no velocity correlations. Recently we have reported[14] that surface impact-induced multifragmentation of a large molecular system can be a fully correlated event. By measuring field-free kinetic energy distributions (KEDs) of C_n^- ($n=1-12$) fragments following collisions of 300–900 eV C_{60}^- ions with a gold surface we have observed the transition from multifragmentation with common average energy for all fragments ("during-collision event") to a one with a common average velocity for all fragments ("post collision event"). KEDs for both multifragmentation modes were successfully treated within a "precursor mediated statistical multifragmentation" model. The actual disintegration stage was described as an expansion/evaporation process of C_n groups off an outgoing precursor which occurs either away from the surface (for near-grazing incidence) or at the surface (for near-normal incidence). It should be noted that during the last two decades C_{60} turned to be a model system for probing the decay dynamics of a highly energized large molecular system with emphasize on distinct fragmentation domains.[15] Recent interest is focused on charge exchange and fragmentation in grazing incidence collisions[14,16–18] Here we extend the validity of the fully velocity correlated multifragmentation mechanism for the impact of C_{60}^- with a nickel target

using not only KEDs of the outgoing C_n^- fragments but also based on the observation of a new effect of gradual narrowing of incidence angle dependences of the C_n^- fragment yield as a function of the fragment size n. This effect is analyzed in terms of a precursor mediated, statistical (expansionlike) multifragmentation mechanism resulting in a predicted $1/\sqrt{n}$ narrowing law which is found to be in good agreement with the experimental results.

II. EXPERIMENTAL

Only a brief description of the setup will be given here focusing on the most relevant experimental aspects. A more detailed report was given earlier.[19,20] C_{60}^- anions were generated by passing the fullerene vapors through heated ceramic capillary combined with soft (thermal) electron attachment/pickup. This results in highly mass pure (99.99%) C_{60}^- ion beam (no need for any mass filtering) with narrow energy width ($\leq$0.6 eV) as measured using an on-line mass filter equipped with a retarding field energy analyzer. The C_{60}^- ions were collided at kinetic energies of 200–900 eV with sputtered/annealed atomically clean polycrystalline nickel surface maintained under under ultra high vacuum conditions. In order to assure surface cleanness, avoid C_{60} sticking and generally maintain stable surface conditions, surface temperature was kept at 950 K throughout all measurements. All the mass resolved energy and angle distributions are highly reproducible with no sign for any gradually accumulated surface damage. Surface quality (smoothness and flatness) is demonstrated by the near-specular incidence angle dependences. The experimental configuration is that of a rotating surface and a fixed detector such that the scattering angle is given by $\Psi=\pi-(\theta_i+\theta_r)$ with incidence angle θ_i and reflection angle θ_r both defined with respect to the surface normal. A near-grazing ($\Psi=45°$) configuration was employed in the experiments reported here. The detected signal is therefore confined within the $\theta_i=45-90$ range. Mass resolved KEDs and incidence angle dependences $I_n(\theta_i)$ of outgoing C_n^- fragments were measured by a mass-spectrometer equipped with on-axis retarding field energy analyzer (ΔE =0.4 eV). All KEDs and $I_n(\theta_i)$ dependences were measured under completely field-free conditions. All elements including sample holder, heater and electrical leads and flight path of the fragment ions from the surface to the energy analyzer were fully screened.

III. RESULTS AND DISCUSSION

A. Multifragmentation yield curve

At impact energies above 200 eV the scattered beam mass spectrum was dominated by small odd/even (n numbered) C_n^- fragments—a well-established characteristic of the fullerene multifragmentation regime ($n=2-23$ for $E_0=300$ eV and $n=2-18$ for $E_0=600$ eV). Figure 1 presents the total (mass and energy integrated, normalized over primary beam current) yield of the C_n^- fragment ions for C_{60}^- impact energies of 200–900 eV. The very steep rise followed by a plateau region demonstrates a clear shattering-type transition resembling a first-order phase transition caloric (temperature-energy) curve. The signal grows up by about a factor of 100 starting from a threshold value at $E_0=200$ eV till $E_0=400$ eV followed by a rather sharp transition to a plateau region beyond 500 eV (over the $E_0=500-900$ eV range measured here). According to our "precursor mediated multifragmentation" model,[14] the C_n^- fragments are produced by the decay of a very highly vibrationally excited precursor ion. The precursor ion is assumed to be a superhot ensemble of 60 carbon atoms which are temporally organized into a cluster of C_n groups, loosely interconnected but tightly confined. The incoming C_{60}^- is probably fully neutralized upon impact, along the entrance leg of the scattering trajectory. A small fraction of the neutralized projectiles reionizes via surface electron pickup along the exit trajectory resulting in an outgoing singly charged precursor anion. The absolute yield indicated in Fig. 1 is mostly due to the relatively low (0.1–0.3 %) reionization probability. This precursor anion can now thermionically emit the excess electron (thus avoiding detection as an ion) or multifragments into several neutral C_n fragments and a negatively charged one. Since we are detecting only negative ions, each of the counted C_n^- fragments is originating from a different precursor ion while all other neutral C_n fragments are not detected. The mass integrated C_n^- yield curve in Fig. 1 is therefore reflecting the net increase in negatively charged precursor ions as a function of impact energy. The total C_n yield, including neutrals, is probably increasing even more steeply. The plateau region reflects saturation in the formation rate of appropriate precursor ions or some steady state between rate of precursors formation and rate of some suppressing decay process such as thermionic emission preceding multifragmentation, based on different internal energy dependence of each of the competing rates.

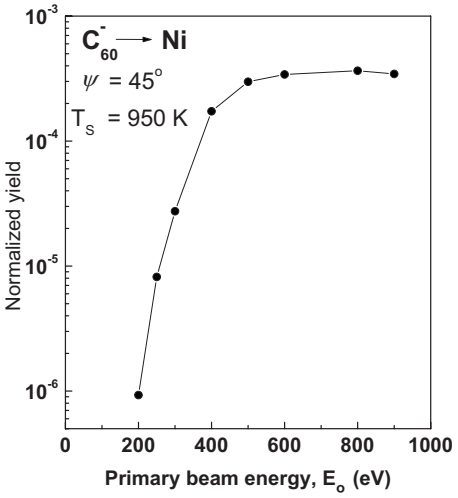

FIG. 1. Multifragmentation yield curve (total yield of C_n^-) for near grazing ($\Psi=45°$) C_{60}^- impacting a nickel surface at 200–900 eV. The yield is normalized over primary beam current.

B. Kinetic energy distributions

The measured mass-dependent KEDs for the outgoing C_n^- ($n=2-10$) ions are presented in Fig. 2 (dots) along with the calculated distributions (thin solid line). As before (for the

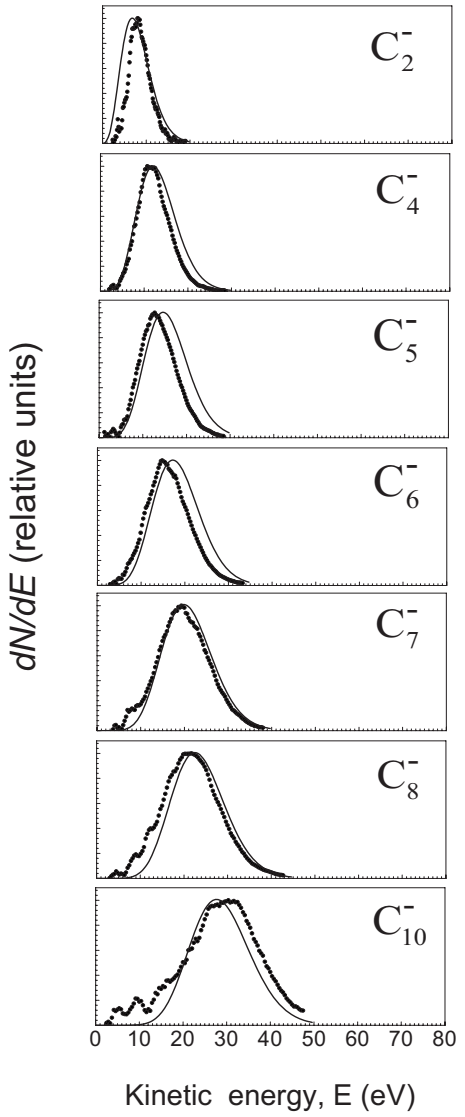

FIG. 2. Kinetic-energy distributions of outgoing C_n^- fragment ions following impact of C_{60}^- ion on a nickel surface at kinetic energy $E_0=600$ eV and near-grazing incidence ($\Psi=45°$, $\theta_i=61°-62°$). Both measured (dots) and calculated (thin solid lines) distributions are shown. All calculated shifted Maxwell distributions are given by Eq. (1) with a single pair of best fitted parameters $kT=0.86$ eV and $\varepsilon=2.60$ eV. All distributions are normalized to the same peak intensity.

Au target[14]) the complete KEDs family of C_n^- fragments was successfully and uniquely fitted by a shifted Maxwellian flux distribution

$$\frac{dN_n}{dE} \propto E \exp\left(-\frac{(\sqrt{E}-\sqrt{n\varepsilon})^2}{kT}\right) \quad (1)$$

characterized by only two parameters: the precursor center-of-mass velocity $V_{\text{c.m.}}$ (or corresponding kinetic energy $\varepsilon = mV_{\text{c.m.}}^2/2$ of a single carbon atom with mass m) and its temperature T (k is the Boltzmann constant). The best fitted parameters used for the calculated distributions as given in Fig. 2 are $kT=0.86$ eV and $\varepsilon=2.60$ eV. Note the good agreement which provide confidence in the concept of statistical multifragmentation of a nearly thermally equilibrated moving precursor ion. The temperature T is used in the sense of a microcanonical temperature (defined for a single, isolated precursor species serving as its own heat bath). The fact that it qualifies as a characteristic parameter which describes rather well the very short-time scale (estimated to be subpicosecond) multifragmentation event is a manifestation of the momentary high density attained within the precursor ion upon surface impact. The fitted T value also reflects an ensemble average over a distribution of outgoing precursors (each with its own fixed, impact deposited, internal energy). The good agreement obtained between experimental KEDs and the shifted Maxwellian distribution shows that the distribution of internal energies between the different precursors is rather narrow and the microcanonical temperature is therefore nearly the same as the ensemble averaged one. Similar arguments regarding $V_{\text{c.m.}}$ lead to the conclusion that the distribution of kinetic energies of the outgoing precursors is rather narrow as well. The values of the fitted parameters imply $60\times\varepsilon=156$ eV kinetic energy of outgoing precursor (74% primary ion kinetic-energy loss) and internal vibrational excitation which is given by $E_v^{eff}\equiv\overline{E_v}-\text{ZPE}=140$ eV, where $\overline{E_v}=174kT=149.6$ eV and ZPE=9.7 eV is the zero-point energy (ZPE) (estimated as for C_{60}).[21] From total-energy balance one gets 304 eV energy transfer to the surface. Note that even the extreme vibrational excitation as extracted here is still considerably lower than the total cohesion energy of C_{60} ($\sim$450 eV).[22]

A different, explosionlike, multifragmentation scenario for ion impact excited fullerenes was proposed by Cheng *et al.*[23] (high-energy collisions with multicharged xenon ions) and Rentenier *et al.*[24] (medium energy collisions with singly charged light ions). By analyzing time-of-flight (TOF) line shapes of C_n^+ ($n=1-12$) fragments they have extracted nearly constant fragment ions momentum value P_{TOF}, which corresponds to $1/n$ scaling of the most probable energies E_{mp} of these ions (in c.m. frame). They have associated this surprising observation with an explosive type multifragmentation of a multicharged fullerene. However, there is no fundamental physical reasoning supporting the description of the explosive multifragment break up as a constant momenta event. For our thermally equilibrated precursor case, the average thermal momenta $\langle P_{kT}\rangle=\sqrt{8kTmn/\pi}$ of C_n^- fragments (in the c.m. frame of the precursor ion) is proportional to $\sqrt{n}$. It is interesting to note that the constant momentum value of $P_{\text{TOF}}\approx 135$ a.u. found by Rentenier *et al.*[24] for C_n^+ fragments with $n>6$ is comparable with the range of average momentum value $\langle P_{kT}\rangle=94-162$ a.u. for $n=5-15$ in our experiment.

C. Incidence angle dependences—width narrowing effect

The nature of the evaporation/expansion process of the moving precursor should be reflected also in the angular distributions of the emitted C_n^- fragments. Figure 3 shows the incidence angle dependences $I_n(\theta_i)$ as a function of the fragment size n. The width [full width at half maximum (FWHM) value] of these dependences is decreasing monoto-

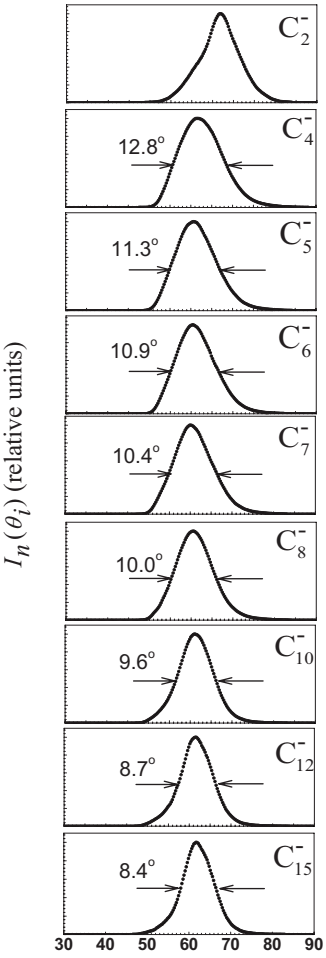

FIG. 3. Incidence angle dependences $I_n(\theta_i)$ of outgoing C_n^- fragment ions following impact of C_{60}^- ion on a nickel surface at kinetic energy E_0=600 eV and near-grazing incidence (Ψ=45°). Note the gradual narrowing of the width (FWHM value).

nously from a value of 12.8° for C_4^- to 8.4° for C_{15}^-. Due to improved signal-to-noise ratio for the angular (integrated) dependences as compared with the KEDs we were able to get good quality measurements down to n=15.

We assume that the width of the $I_n(\theta_i)$ dependence of shattered ions intensities indirectly represent that of the angular distribution $J_n(\theta_r, \theta_i$=const.) of fragment ions emitted at an angle θ_r relative to the surface normal. We also assume that for an incidence angle $\theta_i^{\max}$ [maximum of the $I_n(\theta_i)$ dependence], the emission direction corresponding to the angle $\theta_r^{\max}$ [maximum of the $J_n(\theta_r, \theta_i$=const.) distribution] coincides with the direction of detection of the fragment ions such that $\theta_r^{\max}=\pi-\Psi-\theta_i^{\max}$. For the near-grazing scattering configuration (Ψ=45°) the value of $\theta_i^{\max}\approx 61°-62°$ is smaller than the specular value 67.5° by only a few degrees. The same result was found for the case of the near-normal scattering configuration (Ψ=135°) for which $\theta_i^{\max}\approx 20°$ as compared with the specular value of 22.5°. Taking into account this similarity along with the experimental condition $\theta_i+\theta_r$=const., one can conclude that some arbitrary deviation $\Delta\theta_i$ of the incidence angle from the value of $\theta_i^{\max}$ results in a corresponding deviation of the registration direction from $\theta_r^{\max}$ by the value of $\Delta\theta_r\approx -2\Delta\theta_i$ (see also Ref. 25).

Our model assumes that the thermalized precursor which is leaving the surface is the source for the emitted fragments. Within this statistical model, the velocity directions of the various fragments are isotropic in the center-of-mass frame while in the laboratory frame they define some angle $\beta(n) \ll \pi/2$ with the precursor ion velocity. For the averaged value $\langle\beta(n)\rangle$ one can write

$$\langle\beta(n)\rangle = \text{arctg}\frac{\langle V_\perp(n)\rangle}{V_{\text{c.m.}}} = \text{arctg}\frac{0.5V(n)}{V_{\text{c.m.}}}, \tag{2}$$

where $V(n)$ is the velocity of the C_n^- fragment in the center-of-mass frame and the factor 0.5 at the numerator results from averaging of the in-plane $V_\perp(n)$ component perpendicular to the precursor velocity $[\langle V_\perp(n)\rangle = V(n)\langle\sin\alpha\cos\varphi\rangle]$. Spherical averaging over all possible orientations (random velocity directions) was carried out within the azimuthal angle (φ) interval $[-\pi/2, +\pi/2]$ and polar angle (α, defined with respect to the $V_{\text{c.m.}}$ vector) interval $[0, \pi]$. If $J_{prec}(\theta_r, \theta_i$=const.) is the angular (θ_r) emission distribution of precursor ions relative to the surface normal (in the scattering plane) with a width $\Delta_r(prec)$ then one can expect that the width $\Delta_r(n)$ of the emitted fragment ion distribution $J_n(\theta_r, \theta_i$=const.) (in the same plane) will be larger than $\Delta_r(prec)$ by $\delta_r(n)$ such that

$$\delta_r(n) \equiv \Delta_r(n) - \Delta_r(prec) \approx 2\langle\beta(n)\rangle. \tag{3}$$

Since the $I_n(\theta_i)$ dependence of shattered ions intensities indirectly represents the distribution $J_n(\theta_r, \theta_i$=const.) of emitted fragment ions, one can also introduce the quantity $\delta_i(n)$ defined as

$$\delta_i(n) = \Delta_i(n) - \Delta_i(prec), \tag{4}$$

where $\Delta_i(n)$ is the width of the incidence angle dependence $I_n(\theta_i)$ for the fragment C_n^- ions and $\Delta_i(prec)$ is the corresponding width of $I_{prec}(\theta_i)$ for the precursor ions. The broadening of the $I_{prec}(\theta_i)$ dependence is therefore given by $\delta_i(n)$, which represents the broadening $\delta_r(n)$ of the $J_{prec}(\theta_r, \theta_i$=const.) distribution. Using the angular deviations relation $|\Delta\theta_r| \approx |2\Delta\theta_i|$ (see above), one can conclude that

$$\delta_i(n) = B\frac{\delta_r(n)}{2}. \tag{5}$$

The proportionality factor B is related with the uncertainty of the transition from the measured width of the incidence angle dependence $I_n(\theta_i)$ to the unmeasured width of the $J_n(\theta_r, \theta_i$=const.) distribution. It is also related with some uncertainty of the chosen value of characteristic velocity V in the Maxwellian distribution, responsible for the broadening of the $J_{prec}(\theta_r, \theta_i$=const.) distribution or $I_{prec}(\theta_i)$ dependence. We believe that value of the factor B is of the order of unity.

Using Eqs. (2) and (3) one can now rewrite Eq. (5) as

$$\delta_i(n) = B\ \text{arctg}[0.5V(n)/V_{\text{c.m.}}]. \tag{6}$$

In the center-of-mass frame the most probable speed of fragment ions with mass nm is given by $\sqrt{2kT/nm}$. Since $0.5V(n)/V_{\text{c.m.}} \ll 1$, Eq. (6) can be approximated [for any

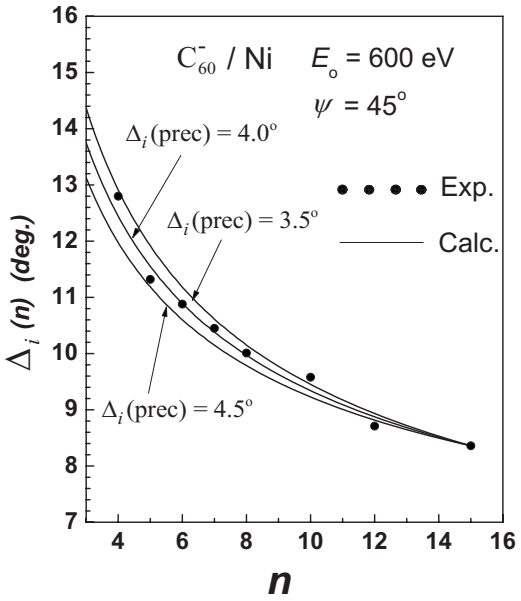

FIG. 4. Measured (dots) and calculated (solid lines) widths $\Delta_i(n)$ of incidence angle dependences $I_n(\theta_i)$ of outgoing C_n^- fragment ions following impact of C_{60}^- ions on a nickel surface at E_0 =600 eV and near-grazing incidence (Ψ=45°). The calculation is based on Eq. (7) using n_{ref}=15 and $\Delta_i(prec)$=4° as a fitting parameter. Fitting sensitivity is demonstrated by plotting calculated curves with ±0.5° deviation of $\Delta_i(prec)$ from the fitted value.

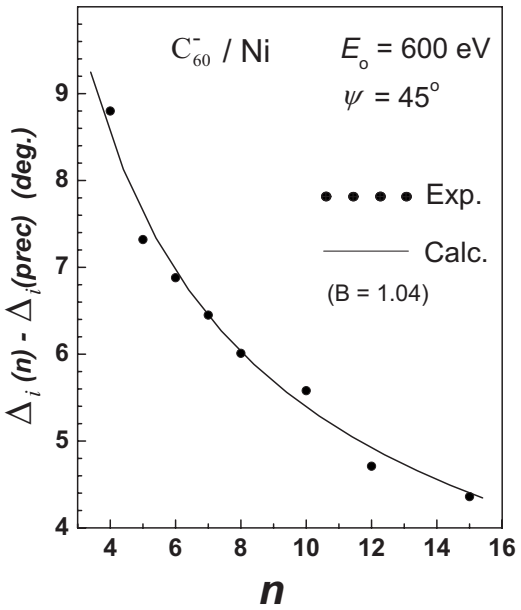

FIG. 5. The differences $\Delta_i(n)-\Delta_i(prec)$ [using experimental widths $\Delta_i(n)$ and $\Delta_i(prec)$=4° as in Fig. 4] plotted as a function of n, together with the corresponding calculated broadening values as given by the right side of Eq. (8): $B\times 0.5\sqrt{kT/n\varepsilon}$ (using kT =0.86 eV and ε=2.60 eV taken from Fig. 2). A best fitted B =1.04 is obtained.

given value of E_o and hence corresponding values of $V_{\text{c.m.}}$ (or $\varepsilon = mV_{\text{c.m.}}^2/2$) and kT] as

$$\delta_i(n) \approx B \times 0.5V(n)/V_{\text{c.m.}} = A/\sqrt{n} \tag{7}$$

with $A = B \times 0.5\sqrt{kT/\varepsilon}$.

At this stage, using Eqs. (4) and (7) and treating the value of $\Delta_i(prec)$ as a fitting parameter one can try to describe the measured $\Delta_i(n)$ dependence. For this one have to assume B =1, taking kT and ε as extracted from Fig. 2. Instead, we use a different approach enabling us to deduce the $\Delta_i(prec)$ value independently from the B value. Assuming that the value of the coefficient B is not known, we consider the $\Delta_i(n)$ dependence relative to some reference value $n=n_{ref}$

$$\Delta_i(n) = \sqrt{\frac{n_{ref}}{n}}[\Delta_i(n_{ref}) - \Delta_i(prec)] + \Delta_i(prec). \tag{8}$$

Figure 4 presents the measured widths $\Delta_i(n)$ of the $I_n(\theta_i)$ dependence of fragment C_n^- ion intensities (taken from the data in Fig. 3) vs the number n of C atoms in the ion for E_0=600 together with $\Delta_i(n)$ dependences calculated by Eq. (8). The value of n_{ref}=15 was used and the fitted value of $\Delta_i(prec)$=4° provides good agreement between calculated and measured dependences. Although the width of the $I_{prec}(\theta_i)$ dependence is not measurable one can compare this result [$\Delta_i(prec)$=4°] with the related width of scattered intact C_{60}^- ions. Unfortunately there is no surviving C_{60}^- at E_0 =600 eV but there is some signal at E_0=100 eV. Indeed, very narrowly peaked and nearly specular $I(\theta_i)$ dependence [$\Delta_i(C_{60}^-)$=3.2°] was measured at E_0=100 eV, lending credibility to the fitted value as deduced here. The correctness of the chosen value of $\Delta_i(prec)$=4° can now be further examined using Eqs. (4) and (7)

$$\Delta_i(n) - \Delta_i(prec) = B \times 0.5\sqrt{kT/n\varepsilon}. \tag{9}$$

As one can see from Fig. 5, when plotting the difference $\Delta_i(n)-\Delta_i(prec)$ using the measured values of $\Delta_i(n)$ and the value of $\Delta_i(prec)$=4°, together with the calculated right side of Eq. (9) [using the best fitted kT=0.86 eV and ε =2.60 eV ($V_{\text{c.m.}}$=6.47×10^5 cm/s) from Fig. 2] as a function of n, a good agreement is achieved with a fitted factor B=1.04. As was expected (see above) the value of the factor B is indeed close to one.

Thus it can be concluded that the precursor mediated statistical multifragmentation scenario (and resulting $1/\sqrt{n}$ narrowing law) is indeed in line with the experimentally observed width narrowing effect of the C_n^- yield incidence angle dependences. The two different types of mass resolved distributions (energy and angle) observed here, are closely related as they both reflect features of the same fundamental multifragmentation mechanism.

IV. CONCLUSIONS

We have studied multifragmentation of C_{60}^- impacting a nickel target at near-grazing incidence and subkiloelectron volt kinetic energies. The C_n^- fragments abundances (odd/even) and characteristic yield curve (as a function of E_0) clearly demonstrate a multifragmentation behavior. By measuring both (field free, mass resolved) kinetic-energy distributions and incidence angle dependences of the product C_n^-

($n=2-15$) fragment ions we have established the validity of a velocity correlated (in the laboratory system), statistical (in the c.m. system) multifragmentation scenario where the multifragmenting source is an outgoing, nearly-thermally equilibrated negatively charged precursor ion. A narrowing effect of the incidence angle dependence (or angular distribution) of the C_n^- yield was observed. We believe that this is the first report of such an effect in dissociative molecule/cluster—surface scattering. Analysis of the effect shows that it is fully consistent with the kinetic-energy distributions and thus provides an additional finger print of the surface impact-induced multifragmentation event.

ACKNOWLEDGMENTS

The research was supported by grants from the Israeli science Foundation (ISF) and by the German-Israeli Binational James Franck program.

[1] L. Oddershede, P. Dimon, and J. Bohr, Phys. Rev. Lett. **71**, 3107 (1993).
[2] J. P. Bondorf, A. S. Botvina, A. S. Iljinov, I. N. Mishustin, and K. Sneppen, Phys. Rep. **257**, 133 (1995).
[3] B. Borderie and M. F. Rivet, Prog. Part. Nucl. Phys. **61**, 551 (2008).
[4] D. H. E. Gross, Phys. Rep. **279**, 119 (1997).
[5] T. Raz, U. Even, and R. D. Levine, J. Chem. Phys. **103**, 5394 (1995).
[6] T. Raz and R. D. Levine, J. Chem. Phys. **105**, 8097 (1996).
[7] E. Hendell, U. Even, T. Raz, and R. D. Levine, Phys. Rev. Lett. **75**, 2670 (1995).
[8] H. Yasumatsu, S. Koizumi, A. Terasaki, and T. Kondow, J. Chem. Phys. **105**, 9509 (1996).
[9] B. Kaiser, T. M. Berhnhardt, B. Stegeman, J. Opitz, and K. Rademann, Phys. Rev. Lett. **83**, 2918 (1999).
[10] P. G. Schultz and L. Hanley, J. Chem. Phys. **109**, 10976 (1998).
[11] J. Laskin, T. H. Bailey, and J. H. Futrell, J. Am. Chem. Soc. **125**, 1625 (2003).
[12] R. D. Beck, C. Warth, K. May, and M. M. Kappes, Chem. Phys. Lett. **257**, 557 (1996).
[13] R. D. Beck, J. Rockenberger, P. Weis, and M. M. Kappes, J. Chem. Phys. **104**, 3638 (1996).
[14] A. Kaplan, A. Bekkerman, B. Tsipinyuk, and E. Kolodney, Phys. Rev. B **79**, 233405 (2009).
[15] E. E. B. Campbell, *Fullerene Collision Reactions* (Kluwer Academic, London, 2003).
[16] S. Wethekam and H. Winter, Phys. Rev. A **76**, 032901 (2007).
[17] S. Wethekam, H. Winter, H. Cederquist, and H. Zettergen, Phys. Rev. Lett. **99**, 037601 (2007).
[18] T. Matsushita, K. Nakajima, M. Suzuki, and K. Kimura, Phys. Rev. A **76**, 032903 (2007).
[19] A. Kaplan, A. Bekkerman, E. Gordon, B. Tsipinyuk, M. Fleischer, and E. Kolodney, Nucl. Instrum. Methods Phys. Res. B **232**, 184 (2005).
[20] A. Bekkerman, A. Kaplan, E. Gordon, B. Tsipinyuk, and E. Kolodney, J. Chem. Phys. **120**, 11026 (2004).
[21] B. Tsipinyuk, A. Budrevich, M. Grinberg, and E. Kolodney, J. Chem. Phys. **106**, 2449 (1997).
[22] M. S. Dresselhaus, G. Dresselhaus, and P. C. Eklund, *Science of Fullerenes and Carbon Nanotubes* (Academic Press, New York, 1996).
[23] S. Cheng, H. B. Berry, R. W. Dunford, H. Esbensen, D. S. Gemmell, E. P. Kanter, T. LeBrun, and W. Bauer, Phys. Rev. A **54**, 3182 (1996).
[24] A. Rentenier, D. Bordenave-Montesquieu, P. Moretto-Capelle, and A. Bordenave Montesquieu, J. Phys. B **36**, 1585 (2003).
[25] A. Bekkerman, B. Tsipinyuk, S. Verkhoturov, and E. Kolodney, J. Chem. Phys. **109**, 8652 (1998).